JACS
JOURNAL OF THE AMERICAN CHEMICAL SOCIETY

ARTICLE

pubs.acs.org/JACS

Rational Design of Ratiometric Near-Infrared Fluorescent pH Probes with Various pK_a Values, Based on Aminocyanine

Takuya Myochin,[†,‡,∥] Kazuki Kiyose,[†,‡,∥] Kenjiro Hanaoka,[†,‡] Hirotatsu Kojima,[‡,§] Takuya Terai,[†,‡] and Tetsuo Nagano*[,†,‡]

[†]Graduate School of Pharmaceutical Sciences, The University of Tokyo, 7-3-1 Hongo, Bunkyo-ku, Tokyo 113-0033, Japan

[‡]CREST, JST, Sanbancho-blg, 5 Sanbancho, Chiyoda-ku, Tokyo, 102-0075, Japan

[§]Chemical Biology Research Initiative, The University of Tokyo, 7-3-1 Hongo, Bunkyo-ku, Tokyo 113-0033, Japan

Supporting Information

ABSTRACT: Novel ratiometric, near-infrared fluorescent pH probes with various pK_a values have been designed and synthesized on the basis of aminocyanine bearing a diamine moiety, and their photochemical properties were evaluated. Under acidic conditions, these pH probes showed a 46- to 83-nm red shift of the absorption maximum. This change is sufficiently large to permit their use as ratiometric pH probes, and is reversible, whereas monoamine-substituted aminocyanines showed irreversible changes because of their instability under acidic conditions. Furthermore, the pK_a values of these probes can be predicted from the calculated pK_a values of the diamine moieties, obtained from the SciFinder database. This design strategy is very simple and flexible, and should be applicable to develop NIR pH probes for various applications.

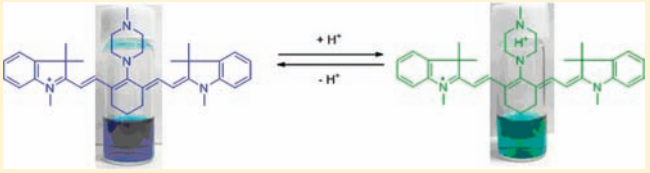

INTRODUCTION

Intracellular or extracellular pH is influenced by diverse physiological and pathological processes, so quantitatively measuring pH is useful for cellular analysis or diagnosis. For example, an acidic environment may be associated with inflammation or tumor.[1] So far, many pH probes have been developed, and some are commercially available.[2−4] However, most of them consist of fluorophores that absorb and emit in the visible region, and there are few near-infrared (NIR) pH probes.[5] Some reviews mention that the range of NIR light especially suitable for In Vivo imaging is 650−900 or 700−1000 nm,[6−8] while the visible light region is generally 400−750 nm.[9] NIR fluorophores, such as tricarbocyanine dyes, have the advantage that light in the NIR region (around 650−900 nm) is relatively poorly absorbed by biomolecules, so it can penetrate deeply into tissues. There is also less autofluorescence in this region, and the characteristics of these dyes are favorable for In Vivo imaging.[6,7] Thus, NIR pH probes based on tricarbocyanine are expected to be suitable for monitoring pH change In Vivo.

Some NIR pH probes, which can detect acidic environments, have been reported so far. Most of them are based on nordicarbocyanine or nortricarbocyanine, and they become highly fluorescent when the protonatable amino group within the fluorophore is protonated.[10−13] Recently, we reported that the excitation wavelength of amine-substituted tricarbocyanine could be modulated by controlling the electron-donating ability of the amine substituent, and we further utilized this phenomenon to develop a ratiometric NIR probe for Zn^{2+} ion.[14] Furthermore, we also developed a ratiometric NIR fluorescent pH probe using this pH response of aminocyanines.[15] However, the fluorescence change of this pH probe is irreversible, which can be problematic.[16] For example, due to this irreversibility, aminocyanines containing a monoamine moiety cannot monitor reversible pH changes in living organs. Therefore, for the development of reversible ratiometric pH probes, aminocyanines that are stable even in acidic environments are required.

RESULTS AND DISCUSSION

pH Dependency of Aminocyanines. We hypothesized that when a proton is delocalized at two nitrogen atoms of aminocyanines bearing a diamino moiety under acidic conditions, such aminocyanines would be stable (Scheme 1). We previously reported that amidation of aminocyanine induced a drastic red-shift in absorption,[15] and this suggests that when protonation occurs at the two nitrogen atoms of such aminocyanines, it would lead to a red-shift of the absorption peak owing to the decrease of the electron-donating ability of the amine. Therefore, we focused on aminocyanines containing ethylenediamine or piperazine moiety as a diamine moiety. Indeed, we designed and synthesized

Received: August 16, 2010
Published: February 22, 2011

dx.doi.org/10.1021/ja1063058 | J. Am. Chem. Soc. 2011, 133, 3401–3409

Scheme 1. Mechanism of pH Response by Protonation and Deprotonation of Aminocyanine Derivatives

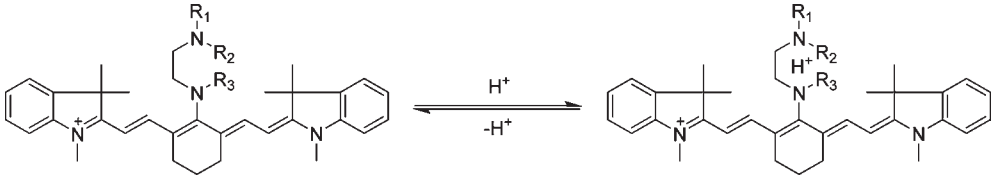

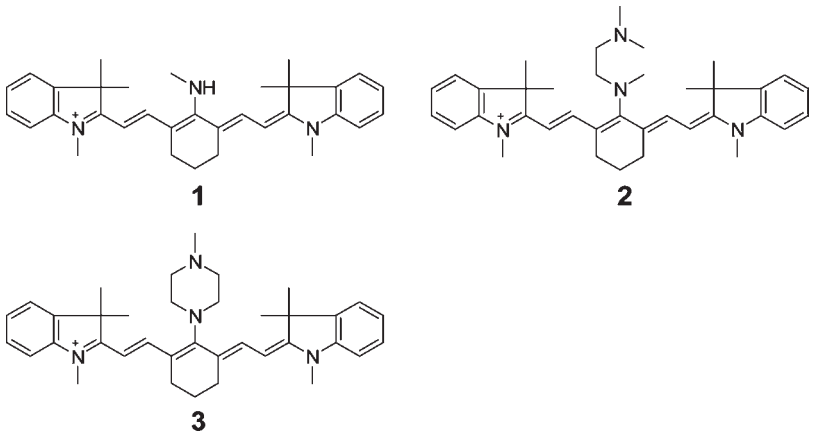

Figure 1. Structures of aminocyanines derivatives **1**, **2**, and **3**.

Scheme 2. Synthetic Scheme for Compounds 2−6[a]

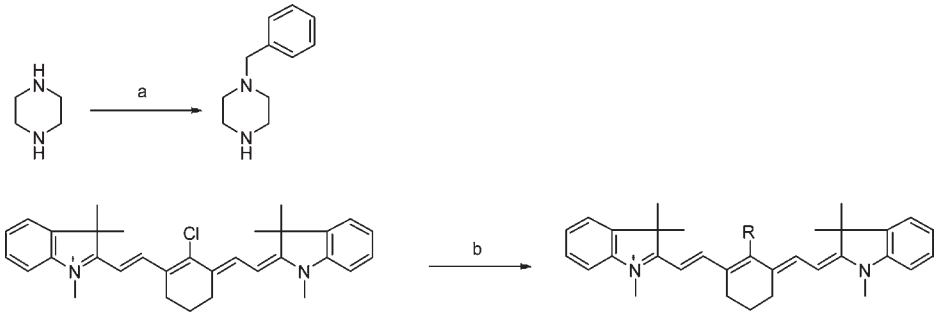

[a] Reagents and conditions: (a) benzyl bromide, dichloromethane, r.t., y. 37%; (b) corresponding amine (R), DMF: R = *N*,*N*,*N*′-trimethylethylenediamine (**2**), r.t., y. 95%; *R* = *N*-methylpiperazine (**3**), r.t., quant.; *R* = *N*,*N*-diethyl-*N*′-methylethylenediamine (**4**), 80 °C, y. 97%; *R* = piperazine (**5**), r.t., y. 99%; *R* = *N*-benzyl piperazine (**6**), r.t., y. 86%.

our previously reported methylamine-substituted aminocyanine (**1**) as a representative of the monoamine type, and novel aminocyanines containing *N*,*N*,*N*′-trimethyl ethylenediamine (**2**) and *N*-methyl piperazine (**3**) as representatives of the diamine type (Figure 1 and Scheme 2), and we examined the pH dependence of their spectral characteristics. Compounds **2** and **3** showed red shifts of 53 and 80 nm of the absorption maximum under acidic conditions, respectively (Figures 2 and 3), while the emission maximum and fluorescence quantum efficiency hardly changed upon protonation or deprotonation (Table 1). Further, we checked the effects of temperature, 10% DMSO and ionic strength on the pH-sensing properties of **8**, which is water-soluble (Figures S1, S2, and S3, and Table S1 of the Supporting Information). The effects seemed to be negligible. These characteristics are favorable for ratiometric pH probes.

Reversibility of the Change in Absorption Spectrum. We further investigated whether **3** is stable in an acidic environment, compared to **1**, which contains a monoamine receptor for H^+ (Figure 4). In agreement with previous findings,[15,16] the NIR absorption of aminocyanine containing a monoamine moiety (**1**) was irreversibly diminished under acidic conditions (Figure 4A, B). This irreversible blue shift in the absorption spectrum was observed during 60 min. However, the NIR absorption of **3** hardly decreased during 60 min, and its spectral change was reversible (Figure 4C,D and 5). This result indicates that **3** is stable even under acidic conditions. From these results, we concluded that it is possible to develop reversible, ratiometric pH probes based on diamine-bearing aminocyanines.

Correlation between Measured pK_a Values of pH Probes and Calculated pK_a Values of Corresponding Diamines. We further tried to develop pH probes with various pK_a values. We

dx.doi.org/10.1021/ja1063058 |*J. Am. Chem. Soc.* 2011, 133, 3401–3409

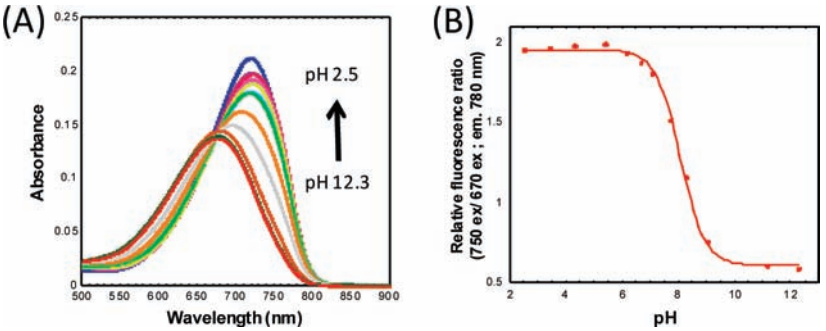

Figure 2. (A) Absorption spectra of 2 μM **2**. All samples were measured in sodium phosphate buffer at pH 2.5, 3.5, 4.3, 5.4, 6.2, 6.7, 7.1, 7.8, 8.3, 9.1, 11.2, and 12.3 in the presence of 10% DMSO as a cosolvent. Emission wavelength is 760 nm. (B) Changes in fluorescence ratio of **2** (750-nm excitation/670-nm excitation, 780-nm emission) in sodium phosphate buffer at the same pH values. The pK_a value of **2** was 8.1.

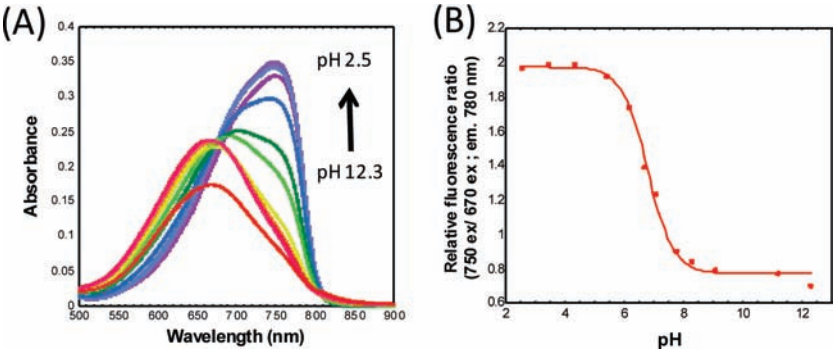

Figure 3. (A) Absorption spectra of 3 μM **3**. All samples were measured in sodium phosphate buffer at pH 2.5, 3.4, 4.3, 5.4, 6.2, 6.7, 7.1, 7.8, 8.3, 9.1, 11.2, and 12.3 in the presence of 10% DMSO as a cosolvent. Emission wavelength is 760 nm. (B) Changes in fluorescence ratio of **3** (750-nm excitation/670-nm excitation, 780-nm emission) in sodium phosphate buffer at the same pH values. The pK_a value of **3** was 6.8.

Table 1. Photochemical Properties of pH Probes Based on the Aminocyanine Scaffold

compound[a]	abs$_{max}$ (nm)	Em$_{max}$ (nm)	extinction coefficient ($M^{-1}cm^{-1}$)	Q.E.	pK_a
2 (protonated)	723	781	1.1×10^5	0.03	8.1
2 (deprotonated)	676	771	8.8×10^4	0.04	
3 (protonated)	750	789	1.1×10^5	0.03	6.8
3 (deprotonated)	667	781	7.4×10^4	0.04	
4 (protonated)	728	781	1.3×10^5	0.03	8.7
4 (deprotonated)	682	770	9.0×10^4	0.03	
5 (protonated)	730	785	9.0×10^4	0.03	8.1
5 (deprotonated)	660	777	6.0×10^4	0.03	
6 (protonated)	759	789	1.3×10^5	0.03	5.5
6 (deprotonated)	686	781	8.6×10^4	0.04	

[a] Acidic condition was pH 3.6, and basic condition was pH 10.9 (compounds **2**, **4**, and **5**) or pH 9.6 (compounds **3** and **6**).

found that the pK_a value of **2** (8.1) was much larger than that of **3** (6.8) (Figure 2 and 3). We considered that this was due to the difference of protonatable diamine, so we synthesized three more aminocyanine derivatives containing various ethylenediamine or piperazine moieties (compounds **4**−**6**) (Figure 6). Further, we measured their absorption spectra to determine the pK_a values of **4**−**6** (Figure 7). We also searched the pK_a values of the corresponding diamine derivatives, calculated by using Advance Chemistry Development (ACD/Laboratories) Software V8.14 for Solaris, from the SciFinder database. Interestingly, there was a good correlation between the measured pK_a values of the corresponding aminocyanines and the calculated pK_a values of the diamine derivatives (Table 2 and Figure 8). The difference between the measured pK_a values of the corresponding aminocyanines and the calculated pK_a values of the diamine derivatives amounts to about 1.0 pH unit, and this may be derived from the difference of chemical structures, i.e., the diamine moieties were directly conjugated with the cyanine scaffold in the structures of aminocyanines, and diamine derivatives obtained from the SciFinder database do not include the cyanine scaffold. The systematic shift of the measured pK_a values of aminocyanines relative to the calculated pK_a values of diamines from the database is probably due to this difference, i.e., the presence or absence of the cyanine scaffold. Furthermore, the emission

dx.doi.org/10.1021/ja1063058 |*J. Am. Chem. Soc.* 2011, 133, 3401–3409

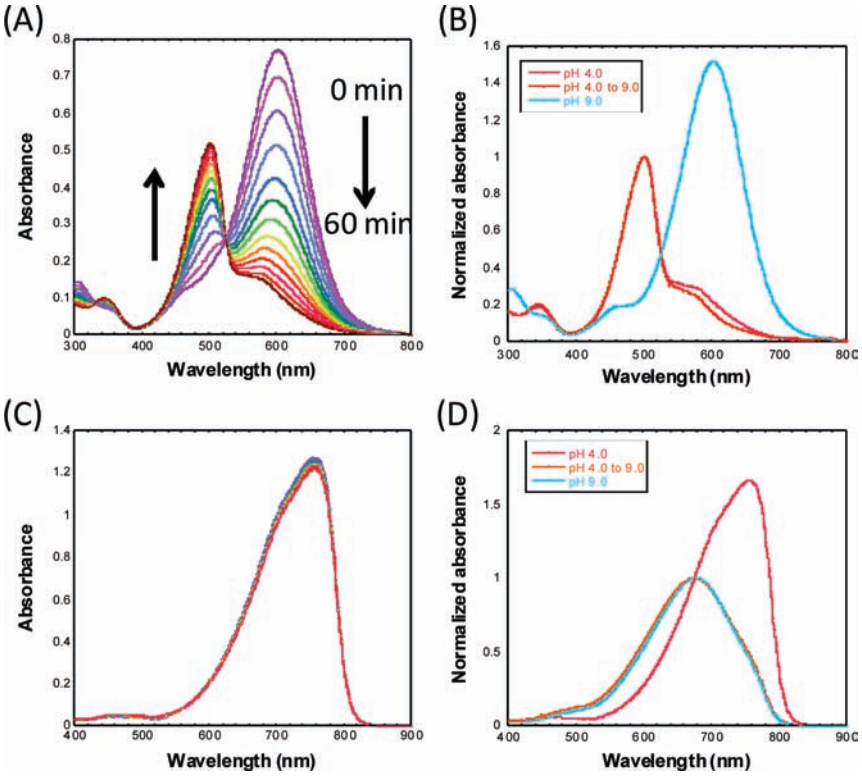

Figure 4. (A,C) Time-dependent changes of absorption of 10 μM **1** (A) or **3** (C) at pH 4.0 during 60 min. (B,D) Investigation of the reversibility of the change for **1** (B) or **3** (D). The absorption spectrum was measured at 60 min after the stock solution of **1** (B) or **3** (D) was dissolved in the buffer (pH 4.0) (red line). After that, the solution was diluted with the buffer (pH 9.0), and the spectrum was measured (yellow line). The spectrum at pH 9.0 is also shown (blue line). All samples were measured in sodium phosphate buffer in the presence of 10% DMSO as a cosolvent.

maximum of each probe hardly changed after protonation, while the absorption maximum markedly changed after protonation (46−83 nm) (Table 1). Namely, ratiometric NIR pH probes with various pK_a values could be rationally designed by referring to the calculated pK_a values of various diamines obtained from the SciFinder database.

For example, if we need a pH probe for sensing an acidic environment, then the pK_a value of aminocyanine can be finely tuned on the basis of the slightly different pK_a values of various diamines. This design strategy is very simple and flexible, and should be applicable to a wide range of ratiometric pH probes for various applications.

Application of pH Probe 7 as a Labeling Agent. For biological and analytical applications, it is often effective to bind a pH probe to macromolecules or carriers to detect certain analytes, which are difficult to detect with typical small sensor molecules.[17−19] Therefore, we synthesized an aminocyanine-based pH probe with a carboxyl group (**7**), which is suitable for labeling (Scheme 3). Its pK_a value was expected to be close to that of **6**, because **7** has a phenyl methyl piperazine moiety. We synthesized latex nano beads conjugated with **7**, and the pK_a value of the nano beads-probe **7** conjugate was determined by measurements of fluorescence intensities. The pH-sensitivity of **7** was retained, but unexpectedly, the pK_a value of the probe in the conjugate (4.2) was much lower than that of **6** (5.5) (Figure 9). It is considered that aliphatic amino groups on the surface of the nano beads might be easily protonated and the resulting cations would influence the protonation efficiency of aminocyanine, decreasing the pK_a value. However, this unexpected pK_a shift is not problematic for our design strategy,

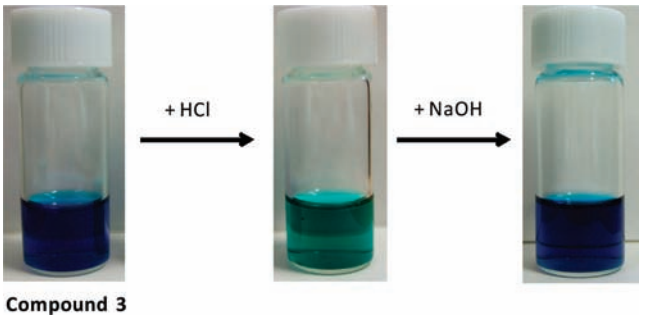

Figure 5. Reversible color changes of compound **3** (methanol solution).

because even if the pK_a value of the pH probe is influenced by carriers or macromolecules, we can still tune the pK_a value of the carrier(or macromolecule)-pH probe conjugate by using the approach described above. Further, we also checked the stability of nano beads-probe **7** conjugate (Figure S4 and Table S2 of the Supporting Information). The nano beads-probe was stable, and the dye molecule was stably immobilized on the nano beads without leakage from the surface for at least a day.

Application of pH Probe 3 for Fluorescence Cellular Imaging. We further investigated the application of **3** in cultured cells (Figure 10). Cultured HeLa cells were incubated with **3** (1 μM) for 10 min at 37 °C. Compound **3** stained mitochondria and lysosomes (Figure S6 of the Supporting Information), and showed a difference of fluorescence ratio between these

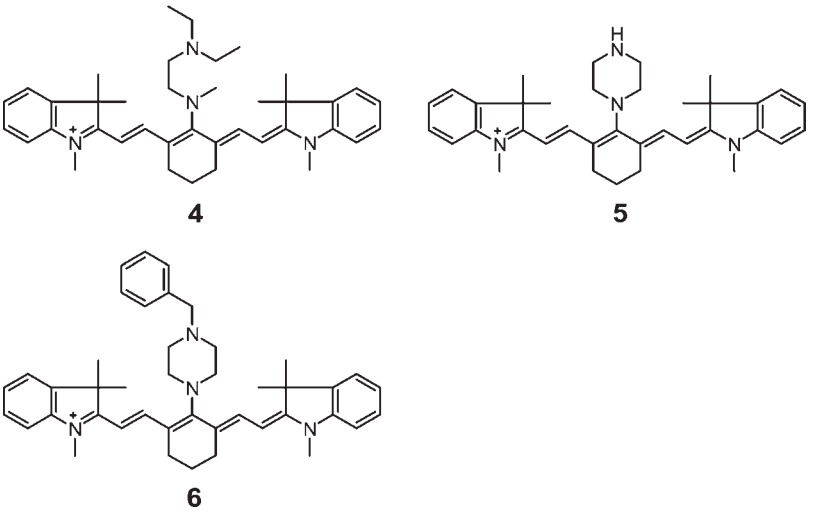

Figure 6. Structures of aminocyanine derivatives **4**, **5**, and **6**.

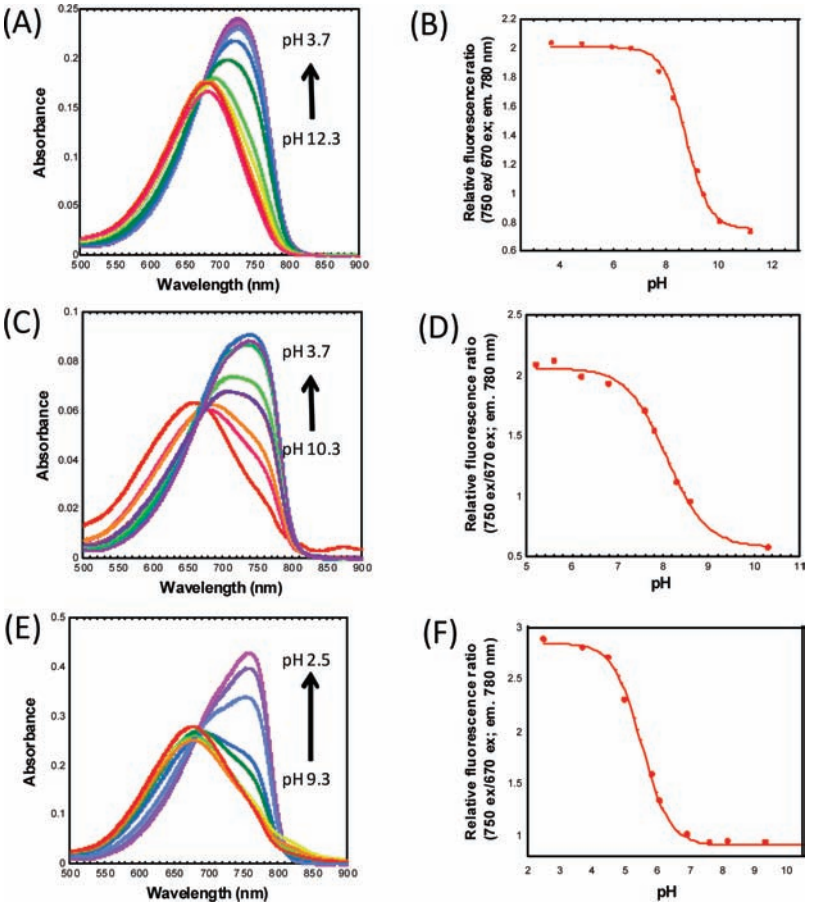

Figure 7. (A,C,E) Absorption spectra of 2 μM **4** (A), 1 μM **5** (C), and 3 μM **6** (E). All samples were measured in sodium phosphate buffer at pH 3.7, 4.8, 6.0, 6.7, 7.8, 8.3, 9.2, 9.4, 10.0, and 12.3 (A), pH 3.7, 5.2, 5.6, 6.2, 6.8, 7.6, 7.8, 8.3, 8.6, and 10.3 (C) or pH 2.5, 3.7, 4.5, 5.0, 5.8, 6.1, 6.9, 7.6, 8.2, and 9.3 (E) in the presence of 10% DMSO as a cosolvent. (B,D,F) Changes in fluorescence ratio of **4** (B), **5** (D), and **6** (F) (750-nm excitation/670-nm excitation, 780-nm emission) in sodium phosphate buffer at the above pH values.

organelles inside the cell (Figure 10B). Next, we added NH_4Cl aq. (final 10 mM) to the cell incubation buffer. It is reported that the pH value of lysosomes changes from pH 4.7−4.8 to 6.2−6.4 inside cells upon addition of NH_4Cl.[20] The fluorescence ratio of lysosomes changed at 1 min after the addition of NH_4Cl, whereas the fluorescence ratio of mitochondria did not change. This result demonstrates that **3** can be used to monitor intracellular pH changes.

dx.doi.org/10.1021/ja1063058 |*J. Am. Chem. Soc.* 2011, 133, 3401–3409

Table 2. Calculated pK_a Values of Diamines and Measured pK_a Values of Diamine-Substituted Aminocyanines

diamine	pK_a of diamine[a]	pK_a of diamine-substituted aminocyanine
N,*N*-diethyl-*N*′-methylethylenediamine (**4**)	10.16	8.7
N,*N*,*N*′-trimethylethylenediamine (**2**)	9.3	8.1
piperazine (**5**)	8.94	8.1
N-methylpiperazine (**3**)	7.83	6.8
N-benzylpiperazine (**6**)	6.31	5.5

[a] Calculated using Advanced Chemistry Development (ACD/Laboratories) Software V8.14 for Solaris (1994−2009 ACD/Laboratories); taken from SciFinder Scholar.

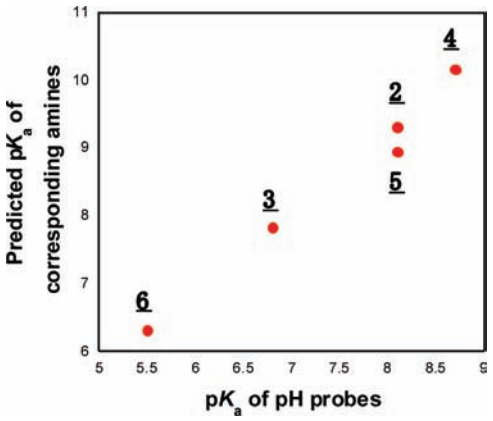

Figure 8. Correlation between pK_a values of pH probes based on aminocyanine (**2**-**6**) and calculated pK_a values of the corresponding diamines, calculated by using Advanced Chemistry Development (ACD/Laboratories) Software V8.14 for Solaris (1994−2009 ACD/Laboratories) as listed in SciFinder Scholar.

CONCLUSIONS

We have established a novel design strategy of pH-induced fluorescence modulation for ratiometric NIR fluorescent pH probes. This approach leads to drastic changes of the absorption or excitation spectra, resulting in large changes of the fluorescence ratio. Furthermore, the pK_a values of such probes can be precisely tuned by referring to the calculated pK_a value of the diamine moiety. A pH probe library designed according to this strategy should be applicable to ratiometric measurement of pH changes over a wide range both in vitro and In Vivo. Synthesis and application of such a library is in progress.

EXPERIMENTAL SECTION

General Procedures. Reagents and solvents were purchased from commercial sources. Reactions were monitored by TLC with visual observation of the dye spots, and by mass spectrometry. Products were purified on a silica gel column, and by semipreparative HPLC. Products were considered pure when a single HPLC peak was obtained.

Instruments. ^{1}H NMR spectra were recorded on a JEOL JNM-LA300. Mass spectra were measured with a JEOL JMS-T100LC mass spectrometer (ESI$^+$ or ESI$^-$). HPLC purification and analyses were performed on a reverse-phase column (GL Sciences (Tokyo, Japan), Inertsil ODS-3 10 × 250 mm for purification and Inertsil ODS-3 4.6 × 250 mm for analyses) fitted on a Jasco PU-1587 system, using eluent A (0.1 M acetic acid/triethylamine buffer (pH 7.4)) and eluent B (CH_3CN with 20% H_2O). The absorbance at 680 nm was monitored for detection. Extinction coefficients were determined using a Shimadzu UV-1600 (Tokyo, Japan). Fluorescence spectroscopic studies were performed with a Hitachi F4500 (Tokyo, Japan). The slit width was 10 nm for both excitation and emission. The photomultiplier voltage was 400 V.

Optical Properties and Quantum Efficiency of Fluorescence. Optical properties of dyes were examined in 0.1 M sodium phosphate buffer (pH 7.4) containing 0.1% (compound **1**) or 10% (v/v) (compounds **2**−**6**) DMSO as a cosolvent, using a Shimadzu UV-1600 UV−vis spectrophotometer and Hitachi F4500 fluorescence spectrophotometer. For determination of the quantum efficiency of fluorescence (Φ_{fl}), cresyl violet in methanol (Φ_{fl} = 0.54) was used as a standard. Values were calculated according to the following equation.

$$\Phi_x/\Phi_{st} = [A_{st}/A_x][n_x^2/n_{st}^2][D_x/D_{st}]$$

where st: standard x, sample; A, absorbance at the excitation wavelength; *n*, refractive index; *D*, area under the fluorescence spectra on an energy scale.

Calculation of pK_a Values. pK_a values of the compounds were calculated by regression analysis of the fluorescence data to fit eq 1.[21] *R* is the ratio of emission intensity at two wavelengths. R_{max} and R_{min} are maximum and minimum limiting values of *R*, and *c* is the slope (positive for the basic forms of the dyes and negative for the acidic forms). I^a/I^b is the ratio of the absorption intensity in acid to the absorption intensity in base at the wavelength chosen for the denominator of *R*.

$$\mathrm{pH} = \mathrm{p}K_a + c\left[\log\frac{R - R_{min}}{R_{max} - R}\right] + \log\frac{I^a}{I^b} \quad (1)$$

Assessment of the Reversibility of the Change in Absorption Spectrum. Compound **1** or **3** was dissolved in 0.1 M sodium phosphate buffer (pH 4.0) containing 10% DMSO as a cosolvent. The absorption spectra of 1 μM **1** or **3** were measured every 10 min from 0 to 60 min (Figure 4). Next, the solvent was diluted to pH 9.0 with 0.1 M sodium phosphate buffer (pH 9.0), and the absorption spectrum was measured again.

Synthetic Protocol for Nano Beads-Probe Conjugate. Nano beads; 20 nm ALIPHATIC AMINE LATEX, 2% W/V (Spherotech)

1 Dilute 2.5 mL aliphatic amine latex microspheres with 10 mL MES buffer (pH 6.0).
2 Centrifuge the mixture to precipitate the particles; 3000 ×*g* for 20 min.
3 Remove supernatant and redisperse pellet in 10 mL MES buffer.
4 Centrifuge again, and remove the supernatant from the particles.
5 Resuspend pellet in 5 mL MES buffer, being sure to completely suspend microsphere particles.
6 To 5 mL of pH probe **7** solution (10 μM) in MES buffer (10 μM), add 2 mM of 50 mg/mL WSCD in MES buffer.
7 Incubate probe/WSCD mixture with gentle mixing at room temperature for 20 min.
8 Take 5 mL of latex in MES buffer solution and add to 5 mL of probe solution.

dx.doi.org/10.1021/ja1063058 |*J. Am. Chem. Soc.* 2011, 133, 3401–3409

Scheme 3. Synthetic Scheme for Compound 7[a]

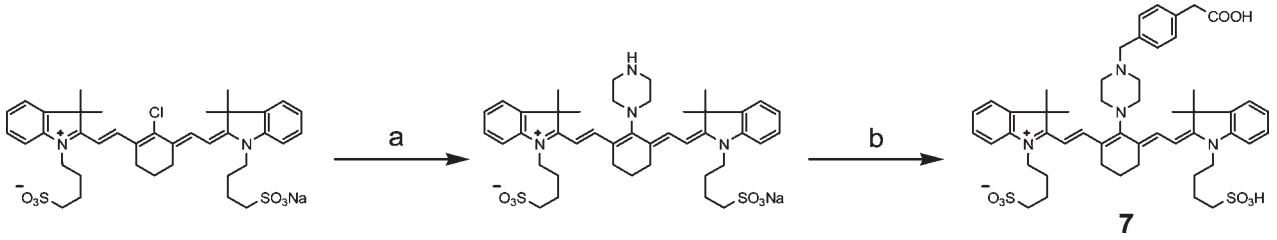

[a] Reagents and conditions: (a) piperazine, DMF, 80 °C; (b) 4-(bromomethyl)phenylacetic acid, DMF, 60 °C.

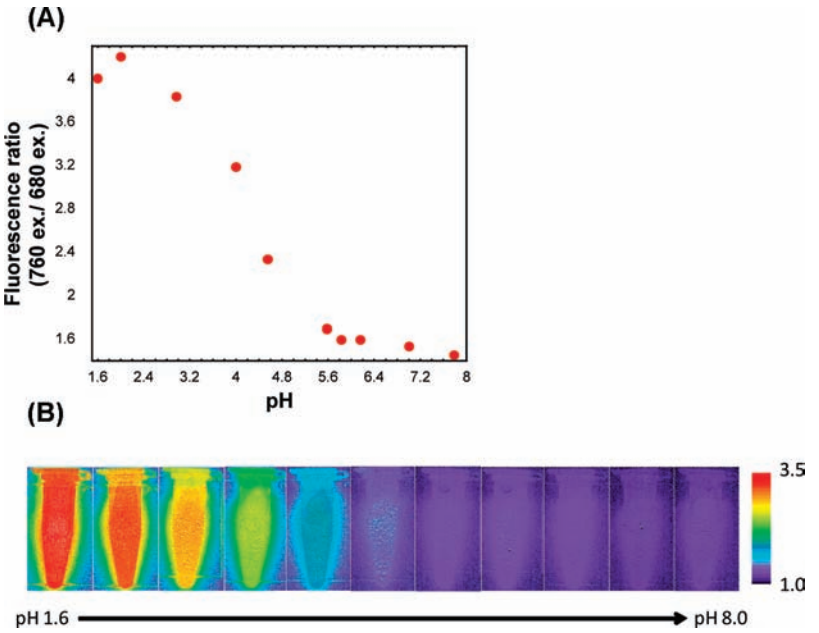

Figure 9. (A) Changes in fluorescence ratio of nano beads-probe 7 conjugate (760-nm excitation/680-nm excitation, over 810-nm emission) in sodium phosphate buffer at pH 1.6, 2.0, 3.0, 4.0, 4.6, 5.6, 5.8, 6.2, 7.0, 7.8, 8.1, and 9.0. Nano beads-probe 7 conjugate was diluted 10-fold with sodium phosphate buffer, and the images were obtained with an imaging device. (B) Ratio images of nano beads-probe 7 conjugate in sodium phosphate buffer at pH.1.6, 2.0, 3.0, 4.0, 4.6, 5.6, 5.8, 6.2, 7.0, 7.8, and 8.1.

9 Incubate latex/probe mixture with gentle mixing at room temperature for 4 h.
10 Remove supernatant, and redisperse pellet in 10 mL PBS.
11 Centrifuge again, and remove the supernatant from the particles (procedure nos. 10 and 11 are repeated 3 times).
12 Resuspend the final latex in 5 mL Storage buffer (PBS; pH 7.4, 0.1% glycine).

Imaging of Nano Beads-Probe Conjugate. Fluorescence images were captured with a Maestro In-vivo Imaging System (CRi Inc., Woburn, MA), with an excitation filter of 680 and 760 nm or 661 and 704 nm, and emission filter of 810 nm long pass or 740 nm long pass, and bright-field settings. Mean fluorescence intensity was measured with Maestro 2.4.0 or 2.10.0.

Preparation of Cells. Hela cells (RIKEN BioResource Center, Japan) were cultured in Dulbecco's modified Eagle's medium (DMEM) (Wako Pure Chemical Industries, Ltd., Osaka, Japan), supplemented with 10% fetal bovine serum (Invitrogen Corp., Carlsbad, CA) and penicillin (100 units/mL)-streptomycin (100 μg/mL) liquid (Invitrogen Corp., Carlsbad, CA) at 37 °C in a humidified incubator containing 5% CO_2 in air.

Ratiometric Imaging of 3 in HeLa Cells. The cells were incubated for 2 days before dye loading on an uncoated 35 mm diameter glass-bottomed dish (D110100, Matsunami, Japan). Then, the cells were rinsed with PBS, incubated with DMEM containing 1% FBS, 1 μM **3**, and 0.1% DMSO as a cosolvent for 10 min at 37 °C, washed with PBS twice, and mounted on the microscope stage.

Ratiometric Imaging System. The ratiometric imaging system comprised an inverted microscope (IX71; Olympus Corp., Tokyo, Japan) and a cooled CCD camera (Cool Snap HQ; Roper Scientific, Tucson, AZ). The microscope was equipped with a xenon lamp (AH2-RX, Olympus), an objective lens (Uapo/340 40×/1.35, Olympus), a dichroic mirror (DM735, Olympus), two excitation filters (IAD MC 660G6, MC 720FX, ASAHI SPECTRA, Japan), and an emission filter (emission filter for Cy7, Olympus). The system was controlled with Metafluor 7.3 software (Universal Imaging, Media, PA).

Fluorescence Confocal Microscopy. Cells seeded on 35-mm glass-bottomed dishes were washed with 1 mL PBS, then incubated in DMEM containing 1% FBS, 1 μM **3**, 5 nM lysotracker green or mytotracker green and 0.2% (v/v) DMSO as a cosolvent for 10 min at 37 °C, washed with 1 mL PBS twice, and mounted on the microscope stage. Fluorescence images were captured using a Leica Application

dx.doi.org/10.1021/ja1063058 |J. Am. Chem. Soc. 2011, 133, 3401–3409

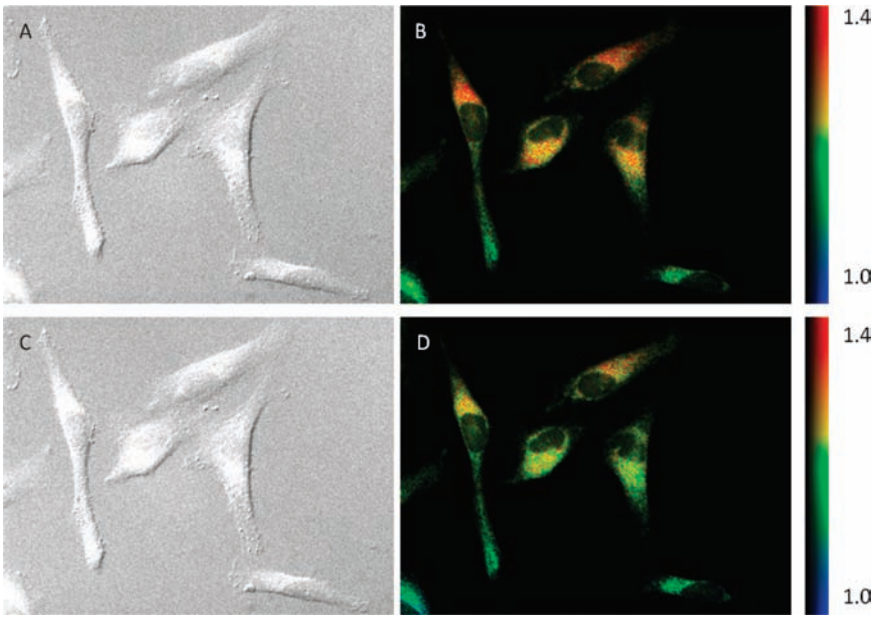

Figure 10. DIC and fluorescence ratiometric images of pH in HeLa cells. HeLa cells were incubated with 1 μM **3** for 10 min at 37 °C, and NH_4Cl aq. (final 10 mM) was added to the medium. (A) DIC image before NH_4Cl aq. was added. (B) Fluorescence ratiometric images with **3** (730 ± 20 nm excitation/660 ± 6 nm excitation, 750−800 nm emission) before NH_4Cl aq. was added. (C) DIC image after NH_4Cl aq. was added. (D) Fluorescence ratiometric images with **3** (730 ± 20 nm excitation/660 ± 6 nm excitation, emission) after NH_4Cl aq. was added.

Suite Advanced Fluorescence (LAS-AF) with a TCS SP5 and a 40× objective lens. The light source was a white-light laser. The excitation wavelength was 448 and 670 nm, and the emission wavelength was 500−530 nm (lysotracker green and mytotracker green), or 700−800 nm (dye **3**), respectively. PMT; Gain: 800 V (lysotracker green and mytotracker green), 550 V (dye **3**) Offset 0%

Synthesis of *N*-Benzylpiperazine. Piperazine (2.2 g, 26 mmol) was dissolved in dichloromethane (20 mL). Benzyl bromide (3.4 g, 13 mmol) was added dropwise to the solution on ice bath. The mixture was stirred at room temperature for 6 h. The solvent was removed under reduced pressure, and then the crude product was purified by silica gel chromatography with dichloromethane to afford a colorless solid (849 mg, 34%). 1H-NMR (300 MHz, $CDCl_3$): δ 2.37 (br, 4H), 2.84 (t, 4H, J = 4.95), 3.46 (s, 2H), 7.18−7.31 (m, 5H,). ^{13}C NMR (75 MHz, $CDCl_3$): δ 45.7, 54.1, 63.3, 126.6, 127.8, 128.8, 137.8. LRMS (ESI^+): m/z 177 ($M + H^+$).

Synthesis of IR786-Methylamine (1). This compound was synthesized following ref 13.

Synthesis of IR786-*N,N,N′*-Trimethylethylenediamine (2). IR-786 perchlorate (60 mg, 0.1 mmol) was dissolved in anhydrous DMF (5 mL), and *N,N,N′*-trimethylethylenediamine (41 mg, 0.4 mmol) was added. The mixture was stirred at room temperature for 3 h under an argon atmosphere. The solvent was removed under reduced pressure, then the crude product was purified by silica gel chromatography with dichloromethane and methanol, and washed with *n*-hexane to afford a glossy blue solid (62 mg, 95%). ^{1}H NMR (300 MHz, CD_3OD): δ 1.54 (s, 12H), 1.69−1.78 (m, 2H), 2.12 (s, 6H), 2.42 (t, 4H, J = 6.6 Hz), 2.64 (t, 2H, J = 6.1 Hz), 3.35 (s, 3H), 3.37 (s, 6H), 3.80 (t, 2H, J = 6.1 Hz), 5.77 (d, 2H, J = 13.4 Hz), 6.98−7.03 (m, 4H), 7.19−7.31 (m, 4H), 7.62 (d, 2H, J = 13.4 Hz). ^{13}C NMR (75 MHz, $CDCl_3$): δ 21.8, 24.1, 28.6, 28.9, 30.5, 44.4, 45.0, 47.7, 57.3, 95.1, 108.8, 121.8, 123.0, 123.2, 128.2, 139.9, 142.1, 143.3, 169.0, 176.1. HRMS (ESI^+) Calcd for [M − ClO_4^-]: 549.3957, found: 549.3967.

Synthesis of IR786-*N*-Methylpiperazine (3). IR-786 perchlorate (60 mg, 0.1 mmol) was dissolved in anhydrous DMF (5 mL), and 1-methylpiperazine (40 mg, 0.4 mmol) was added. The mixture was stirred at room temperature for 3 h under an argon atmosphere. The solvent was removed under reduced pressure, then the crude product was purified by silica gel chromatography with dichloromethane and methanol, and recrystallized from methanol and *n*-hexane to afford a golden powder (66 mg, quant.). ^{1}H NMR (300 MHz, CD_3OD): δ 1.59 (s, 12H), 1.72−1.76 (m, 2H), 2.38 (s, 3H), 2.44 (t, 4H, J = 6.4 Hz, e), 2.66 (br, 4H), 3.42 (s, 6H), 3.67 (t, 4H, J = 4.8 Hz), 5.85 (d, 2H, J = 13.4 Hz), 7.04−7.08 (m, 4H), 7.23−7.35 (m, 4H), 7.69 (d, 2H, J = 13.4 Hz). ^{13}C NMR (75 MHz, $CDCl_3$): δ 21.6, 24.9, 28.8, 30.8, 46.1, 47.9, 54.9, 56.5, 96.2, 109.2, 121.8, 123.4, 124.4, 128.4, 139.9, 141.2, 143.2, 169.3, 173.6. HRMS (ESI^+) Calcd for [M − ClO_4^-]: 547.3800, found: 547.3815.

Synthesis of IR786-*N,N*-Diethyl-*N′*-Methylethylenediamine (4). IR-786 perchlorate (60 mg, 0.1 mmol) was dissolved in anhydrous DMF (5 mL), and *N,N*-diethyl-*N′*-methylethylenediamine (52 mg, 0.4 mmol) was added. The mixture was stirred at room temperature for 3 h under an argon atmosphere. The solvent was removed under reduced pressure, then the crude product was purified by silica gel chromatography with dichloromethane and methanol, and washed with *n*-hexane to afford a glossy blue solid (66 mg, 97%). ^{1}H NMR (300 MHz, $CDCl_3$): δ 1.04 (t, 6H, J = 7.0 Hz), 1.67 (s, 12H,), 1.83−1.87 (m, 2H), 2.48 (t, 4H, J = 6.2 Hz), 2.58 (q, 4H, J = 7.0 Hz), 2.89 (br, 2H), 3.48 (s, 6H), 3.53 (s, 3H), 3.91 (t, 2H, J = 6.1 Hz), 5.73 (d, 2H, J = 13.4 Hz), 6.98 (d, 2H, J = 7.9 Hz), 7.10 (t, 2H, J = 7.43 Hz), 7.29−7.34 (m, 4H), 7.58 (d, 2H, J = 13.4 Hz). ^{13}C NMR (75 MHz, $CDCl_3$): δ 10.9, 21.7, 24.2, 29.1, 30.5, 44.8, 46.6, 47.7, 50.9, 55.2, 95.2, 108.8, 121.8, 123.0, 128.3, 139.9, 141.7, 143.3, 168.8, 175.8. HRMS (ESI^+) Calcd for [M − ClO_4^-]: 577.4270, found: 577.4278.

Synthesis of IR786-Piperazine (5). IR-786 perchlorate (60 mg, 0.1 mmol) was dissolved in anhydrous DMF (5 mL), and piperazine (43 mg, 0.4 mmol) was added. The mixture was stirred at 80 °C for 3 h under an argon atmosphere. The solvent was removed under reduced pressure, then the crude product was recrystallized from 2-propanol to afford a golden powder (62 mg, 99%). ^{1}H NMR (300 MHz, $CDCL_3$): δ 1.67 (s, 12H), 1.81−1.86 (m, 2H), 2.48 (t, 4H, J = 6.42 Hz), 3.27 (br, 4H), 3.50 (s, 6H), 3.90 (br, 4H), 5.74 (d, 2H, J = 13.20 Hz), 6.99 (d, 2H, J = 8.07 Hz),

dx.doi.org/10.1021/ja1063058 |*J. Am. Chem. Soc.* 2011, 133, 3401–3409

7.11 (t, 2H, J = 7.32 Hz), 7.28−7.33 (m, 4H), 7.65 (d, 2H, J = 13.20 Hz). ^{13}C NMR (75 MHz, $CDCL_3$): δ 21.6, 25.3, 28.8, 31.0, 47.0, 48.0, 55.1, 95.8, 109.1, 122.0, 123.4, 123.8, 128.3, 140.0, 140.9, 143.2, 158.0, 169.7. HRMS (ESI^+) Calcd for [M − ClO_4^-]: 533.3644, found: 533.3680.

Synthesis of IR786-*N*-Benzylpiperazine (6). IR-786 perchlorate (60 mg, 0.1 mmol) was dissolved in anhydrous DMF (5 mL), and 1-benzylpiperazine (70 mg, 0.4 mmol) was added. The mixture was stirred at room temperature for 3 h under an argon atmosphere. The solvent was removed under reduced pressure, then the crude product was purified by silica gel chromatography with dichloromethane and methanol, and washed with *n*-hexane to afford a glossy blue solid (62 mg, 86%). ^{1}H NMR (300 MHz, $CDCl_3$): δ 1.62 (s, 12H), 1.78−1.87 (m, 2H), 2.42 (br, 4H), 2.48 (t, 4H, J = 6.4 Hz, f), 3.49 (s, 6H), 3.74 (s, 2H), 3.78 (br, 4H), 5.76 (d, 2H, J = 13.4 Hz), 7.00 (d, 2H, J = 7.8 Hz), 7.12 (t, 2H, J = 7.5 Hz), 7.28−7.40 (m, 7H), 7.59 (d, 2H, J = 13.4 Hz). ^{13}C NMR (75 MHz, $CDCl_3$): δ 21.6, 24.9, 28.8, 30.8, 47.8, 54.1, 55.0, 62.9, 96.0, 109.1, 121.8, 123.4, 124.4, 127.5, 128.4, 128.5, 129.4, 136.6, 139.9, 141.1, 143.2, 169.1, 173.7. HRMS (ESI^+): Calcd for [M − ClO_4^-]: 623.4139, found: 623.4113.

Synthesis of pH Probe 7. IR-783 perchlorate (80 mg, 0.1 mmol) was dissolved in anhydrous DMF (5 mL), and piperazine (43 mg, 0.4 mmol) was added. The mixture was stirred at 80 °C for 1.5 h under an argon atmosphere. 4-Bromophenylacetic acid (275 mg, 1.2 mmol) was added, and stirred at 60 °C under an argon atmosphere overnight. The reaction mixture was poured into 200 mL of diethylether. The precipitate was collected by filtration, and purified by HPLC to afford a blue solid (13 mg, 14%). ^{1}H NMR (400 MHz, CD_3OD): δ 1.53 (s, 12H), 1.70−1.83 (m, 10H), 2.42 (t, 4H, J = 6.40 Hz), 2.72−2.78 (m, 8H), 3.52 (s, 2H), 3.67 (br, 4H), 3.71 (s, 2H), 3.94 (br, 4H), 5.89 (d, 2H, J = 13.20 Hz), 6.79−6.93 (m, 2H), 7.03−7.34 (m, 12H), 7.63 (d, 2H, J = 13.20 Hz). ^{13}C NMR (100 MHz, CD_3OD): δ 23.0, 23.6, 25.8, 26.9, 29.2, 43.0, 44.1, 44.8, 52.0, 55.2, 55.8, 63.4, 97.5, 110.9, 123.2, 124.7, 125.8, 129.6, 130.5, 131.0, 131.1, 135.6, 141.8, 143.0, 144.1, 170.7, 174.6. HRMS (ESI^+) Calcd for [M + H^+]: 925.4243, found: 925.4195.

■ ASSOCIATED CONTENT

Supporting Information. Detailed descriptions of synthetic procedure for **8**; data on the measurements of absorption spectra of **8** with 0.1% or 10% DMSO as a cosolvent, and on the measurements of absorption spectra of **8** in the presence of 500 mM NaCl; plot of the changes of absorbance intensities of **8**; relative fluorescence ratios of **8** at various temperatures; fluorescence intensities of nano beads-probe **7** conjugate after a day; time-dependent changes of absorption spectra of **7**; confocal fluorescence images of live cells. This material is available free of charge via the Internet at http://pubs.acs.org.

■ AUTHOR INFORMATION

Corresponding Author
tlong@mol.f.u-tokyo.ac.jp

Author Contributions
‖These authors contributed equally.

■ ACKNOWLEDGMENT

This work was supported in part by a Grant-in-Aid for JSPS Fellows, by grants from the Ministry of Education, Culture, Sports, Science and Technology of Japan [Grant Nos. 22000006 (Specially Promoted Research) to T.N., 20689001 and 21659204 to K.H.), and by the Industrial Technology Research Grant Program in 2009 from the New Energy and Industrial Technology Development Organization (NEDO) of Japan (to T.T.). K.H. was also supported by Sankyo Foundation of Life Science.

■ REFERENCES

(1) Montcourrier, P.; Mangeat, P. H.; Valembois, C.; Salazar, G.; Sahuquet, A.; Duperray, C.; Rochefort, H. *J. Cell Sci.* **1994**, *107*, 2381–2391.
(2) Cousin, M. A.; Nicholls, D. G. *J. Neurochem.* **1997**, *69*, 1927–1935.
(3) Sun, W. C.; Gee, K. R.; Klaubert, D. H.; Haugland, R. P. *J. Org. Chem.* **1997**, *62*, 6469–6475.
(4) Overly, C. C.; Lee, K. D.; Berthiaume, E.; Hollenbeck, P. J. *Proc. Natl. Acad. Sci. U. S. A.* **1995**, *92*, 3156–3160.
(5) Rurack, K.; Kollmannsberger, M.; Daub, J. *New J. Chem.* **2001**, *25*, 289–292.
(6) Weissleder, R. *Nat. Biotechnol.* **2001**, *19*, 316–317.
(7) Frangioni, J. V. *Curr. Opin. Chem. Biol.* **2003**, *7*, 626–634.
(8) Weissleder, R.; Pittet, M. J. *Nature* **2008**, *452*, 580–589.
(9) Szacilowski, K.; Macyk, W.; Drzewiecka-Matuszek, A.; Brindell, M.; Stochel, G. *Chem. Rev.* **2005**, *105*, 2647–2694.
(10) Encinas, C.; Miltsov, S.; Otazo, E.; Rivera, L.; Puyol, M.; Alonso, J. *Dyes Pigm.* **2006**, *71*, 28–36.
(11) Zhang, Z. R.; Achilefu, S. *Chem. Commun.* **2005**, 5887–5889.
(12) Cooper, M. E.; Gregory, S.; Adie, E.; Kalinka, S. *J. Fluores.* **2002**, *12*, 425–429.
(13) Hilderbrand, S. A.; Weissleder, R. *Chem. Commun.* **2007**, 2747–2749.
(14) Kiyose, K.; Kojima, H.; Urano, Y.; Nagano, T. *J. Am. Chem. Soc.* **2006**, *128*, 6548–6549.
(15) Kiyose, K.; Aizawa, S.; Sasaki, E.; Kojima, H.; Hanaoka, K.; Terai, T.; Urano, Y.; Nagano, T. *Chem.—Eur. J.* **2009**, *15*, 9191–9200.
(16) Yu, Y. H.; Descalzo, A. B.; Shen, Z.; Rohr, H.; Liu, Q.; Wang, Y. W.; Spieles, M.; Li, Y. Z.; Rurack, K.; You, X. Z. *Chem. Asian J.* **2006**, *1*, 176–187.
(17) Ziessel, R.; Ulrich, G.; Harriman, A.; Alamiry, M. A. H.; Stewart, B.; Retailleau, P. *Chem.—Eur. J.* **2009**, *15*, 1359–1369.
(18) Urano, Y.; Asanuma, D.; Hama, Y.; Koyama, Y.; Barrett, T.; Kamiya, M.; Nagano, T.; Watanabe, T.; Hasegawa, A.; Choyke, P. L.; Kobayashi, H. *Nat. Med.* **2009**, *15*, 104–109.
(19) Han, J.; Burgess, K. *Chem. Rev.* **2010**, *110*, 2709–2728.
(20) Ohkuma, S.; Poole, B. *Proc. Natl. Acad. Sci.U. S. A.* **1978**, *75*, 3327–3331.
(21) Whitaker, J. E.; Haugland, R. P.; Prendergast, F. G. *Anal. Biochem.* **1991**, *194*, 330–344.